

Development of the Commercial Manufacturing Process for Ipatasertib

Stephan Bachmann^{§a}, Hans Iding^{§a}, Christian Lautz^{§a}, Isabelle Thomé-Pfeiffer^{§a}, Caroline Maierhofer^{§a}, Régis Mondière^{§a}, Philipp Schmidt^a, Christoph Strasser^{§b}, Thomas Bär^b, André Aebi^b, and Andreas Schuster^{§a*}

[§]Sandmeyer Award 2020

Dedicated to the memory of our colleague Beat Wirz (*30.1.1953 – †31.12.2020)

Abstract: Ipatasertib is a potent small molecule Akt kinase inhibitor currently being tested in Phase III clinical trials for the treatment of metastatic castration-resistant prostate cancer and triple negative metastatic breast cancer. In this paper an overview of the development achievements towards the commercial manufacturing process is given. The convergent synthesis consists of ten steps with eight isolated intermediates and utilizes a wide range of chemical techniques and technologies to build-up this complex drug. All three stereocenters are introduced using enzyme or metal catalysis.

Keywords: Biocatalysis · Catalysis · Drug development · Enzyme · Green chemistry · Metal catalysis



From left to right: Isabelle Thomé-Pfeiffer, Christian Lautz, Hans Iding, Stephan Bachmann, Caroline Maierhofer, Régis Mondière, Andreas Schuster, Philipp Schmidt.

Dr. Isabelle Thomé-Pfeiffer studied chemistry and received a diploma degree from Karlsruhe Institute of Technology, KIT (2008) and PhD from RWTH Aachen University (2013). During her doctoral studies she also joined the group of Bruce H. Lipshutz at UCSB, California. She carried out a postdoctoral study at The Scripps Research Institute, La Jolla, California with P. Baran. In 2015, Isabelle started her career as a process chemist in the department Process Chemistry and Catalysis at F. Hoffmann-La Roche Ltd. Since then, she has worked on several projects from early to late phase development.

Dr. Christian Lautz studied chemistry at the University of Giessen and gained his PhD under the supervision of Prof. Günther Maier

in 1999. After an industrial post-doctoral study at Gödecke AG/Pfizer in Freiburg, Germany, he joined F. Hoffmann-La Roche in Basel, Switzerland, 18 years ago. Since then, he is responsible for process safety work as head of the reaction calorimetry lab, gradually extending the work with projects in the field of PAT. In 2015, Christian joined the Drug Substance Manufacturing Science and Technology (MSAT) team for an internship as plant chemist. Since 2017, Christian and his co-workers are part of the newly established PAT section within the Synthetic Molecules Technical Development department. They design and conduct all PAT projects for drug substance and drug product development, including transfer to and support for Market Manufacturing.

Dr. Hans Iding graduated at the chemistry department of the RWTH Aachen University, Germany in 1995. At the Institute of Enzyme Technology, Heinrich-Heine University Düsseldorf, he worked on the formate dehydrogenase (NADH regeneration) and the benzoyl formate decarboxylase (ThDP dependent carbonylation) receiving his PhD in 1998. He continued his career at Hoffmann-La Roche Basel leading a biotransformation laboratory delivering technical biocatalysis processes and became Senior Principal Scientist. Since 2007, Hans is additionally a chemical project leader. Temporally, he had the lead of the biocatalysis group and was technical project leader. His public work is described in 38 publications and 24 patents.

Dr. Stephan Bachmann obtained his diploma in chemistry (1998) and his PhD from ETH Zurich (2003). After a postdoctoral stay at Aarhus University, Stephan joined the catalysis section of F. Hoffmann-La Roche in 2004, where he is working since then. Stephan's main focus lies on the development and implementation of robust, catalytic processes at technical scale ranging from

*Correspondence: Dr. A. Schuster, E-mail: andreas.schuster.as2@roche.com,

^aDepartment of Process Chemistry & Catalysis, Pharma Synthetic Molecules Technical Development, F. Hoffmann-La Roche AG, Grenzacherstrasse 124, CH-4070 Basel, Switzerland,

^bDottikon Exclusive Synthesis AG, Hembrunnstrasse 17, CH-5605 Dottikon, Switzerland

very early to late phase (clinical) supply. His key expertise lies in the development of catalytic solutions for homogeneous and heterogeneous hydrogenations, carbonylations as well as C–X coupling processes. In recent years, non-noble metal catalyzed processes became a major interest as well.

Dr. Caroline Maierhofer graduated at the chemistry department of the University of Konstanz, Germany, in 2004 and received her PhD in 2009 in the field of bioorganic chemistry. Subsequently, she started her industrial career as an analytical chemist at Carbogen Amcis AG, Switzerland. In 2011, Caroline joined F. Hoffmann-La Roche Ltd. as an analytical development laboratory group leader. In this responsibility, she supported drug substance development projects in early and late clinical phases including initial commercial supply. In 2020, Caroline was assigned as global product owner of a use case within Roche's Digital Transformation Initiative.

Dr. Régis Mondière studied Chemistry and graduated from the Ecole Nationale Supérieure de Chimie de Paris in 2001. He obtained his PhD under the supervision of Dr. C. Mioskowski from the University of Orsay (France) in 2004. After a postdoctoral stay at the Max Planck Institute with Prof. M. T. Reetz (2005), he started his industrial career at Sanofi-Chimie in 2006. He then joined Baxter Pharmaceuticals (2007–2009) and Syngenta Crop Protection AG (2009–2017). Finally he joined F. Hoffmann-La Roche Ltd in 2017 where he is enjoying the development of active pharmaceutical ingredients from early to late development phase.

Dr. Andreas Schuster studied chemistry at the University of Heidelberg, where he also did his PhD in the field of gold catalysis in the group of Prof. Stephen Hashmi. He joined Roche synthetic molecules development in 2012, where he has worked in several functions from process development, over manufacturing, to analytics. Andreas has worked on multiple projects from early to late clinical phases and commercialization. In 2020 he was assigned the role of a section head in process chemistry, where he is also responsible for oligonucleotide process development and digitalization.

Dr. Philipp Schmidt, External Technical Oversight Manager for Pharma Technical Development Small Molecules (PTDC-C) studied chemistry at the University of Würzburg where he also received his doctorate in organic chemistry in 2002. As a post-doc at Novartis (CH-Basel), he developed new targeted contrast agents for *in vivo* imaging studies. At Rohnerchem (CH-Pratteln) Philipp was Group Leader in chemical development and changed in 2009 his role as Technical Project Manager for customer projects. In 2013 he joined Weleda (CH-Arlesheim) as Technical Project Manager Pharmaceuticals. Since 2014 Philipp leads development and manufacturing outsourcing projects of small molecules for clinical supply at Roche.



Dr. Christoph Strasser studied chemistry at the University of Innsbruck, Austria and did his PhD in the Raubenheimer group at Stellenbosch University, South Africa researching gold complexes. After a postdoctoral position in the US at the University of Nevada, Reno in the Catalano group exploring luminescent coinage metal complexes and metallophilic interactions, he started at Dottikon Exclusive Synthesis

and was involved in a part of the presented process development as Senior Project Chemist. His current position is Project Manager Technical Support & PD at Merck & Cie.



Dr. Thomas Bär studied chemistry and completed his PhD at the University of Konstanz (1991). After a postdoctoral fellowship at The Scripps Research Institute, La Jolla, California, Thomas started his industrial career at Byk Gulden/Altana Pharma AG (1992). After years of drug discovery research in various positions at Altana and contributions to the discovery of several preclinical and clinical candidates,

he joined Dottikon Exclusive Synthesis in 2008 as a project manager R&D. In that position, he has been responsible for multiple process development projects throughout all development phases (process design, process development/optimization, transfer to pilot plant and production). Thomas is co/author of 15 papers and 70 patents.



André Aebi studied chemistry and received a diploma FH degree from the University for Applied Sciences, FHBB Muttenz (2008). Afterwards, André started his career as an analytical chemist in the R&D department at Dottikon Exclusive Synthesis, working on the development of analytical methods for several projects. In 2017 he was promoted to senior analytical chemist and leads a team of two analytical chemists and four analytical lab technicians.

1. Introduction

Ipatasertib (**1**) is a potent small molecule Akt kinase inhibitor^[1,2] currently being tested in Phase III clinical trials for the treatment of metastatic castration-resistant prostate cancer and triple negative metastatic breast cancer. Manufacturing of the process performance qualification (PPQ) batches has been completed.

Ipatasertib is a complex molecule with three stereo centers, built up in a ten-step convergent synthesis with eight isolated intermediates (two steps telescoped), using four starting materials, acid **3**, *rac*-**6**, formamidinium acetate, and *N*-Boc-piperazine (Fig. 1). One of the key steps is the coupling of the two main building blocks from the two branches of the synthesis, bicyclic pyrimidine **4** and chiral α -aryl- β -amino acid **2**.

Furthermore, the stereo centers are introduced by highly selective metal and enzyme catalysis (Fig. 2). Ruthenium-catalyzed hydrogenation introduces the stereo center of the β -amino acid moiety, whereas the stereo centers at the cyclopentyl moiety are both formed by enzyme catalysis: a kinetic resolution using a nitrilase and a stereoselective reduction applying a ketoreductase.

Herein, a summary of the development activities with focus on the scale-up work towards the commercial manufacturing process is given, with improved process efficiency and robustness. Details on the route selection can be found in previous publications.^[3–5] Key achievements from the late stage process development are a reduction of the mass intensity (MI in kg per kg API) by factor 5 and an increase of the overall yield by factor 3 over the last three manufacturing campaigns (Fig. 8). Furthermore, the usage of eco-friendly process solvents, solvent regeneration, development of a direct bromination to yield intermediate **5**, upscale of the very sensitive Grignard reaction to intermediate **9**, and a more efficient coupling of the main building blocks **2** and **4** are reported.

2. Synthesis Steps

2.1 Enzymatic Kinetic Resolution of *rac*-**6**

The bicyclic piperazine **9** is manufactured in a four-step synthesis (Scheme 1 – Scheme 4). In the first step, *R*-nitrile **6** is ob-

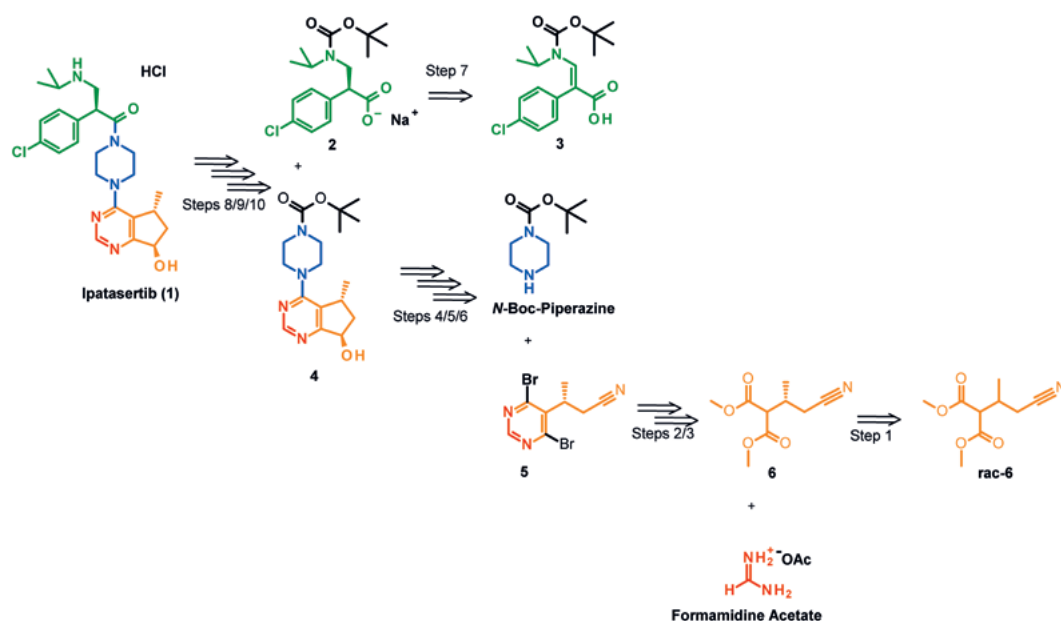


Fig. 1. Structure and Retrosynthesis of Ipatasertib (1).

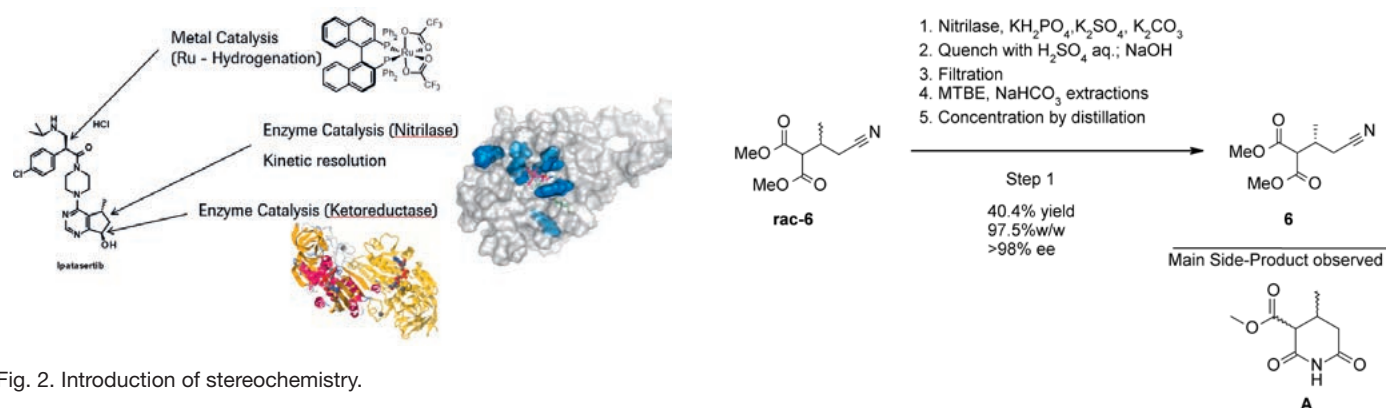


Fig. 2. Introduction of stereochemistry.

tained from **rac-6** by kinetic resolution with a tailor-made engineered nitrilase (Scheme 1). Key achievements on this step were the depletion and control of residual enzyme, and identification of process conditions to limit the formation of side-product **A**.

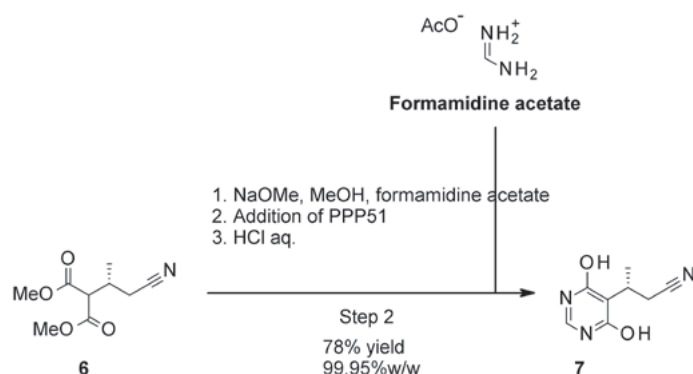
The reaction is run in an aqueous buffer (pH 8.7 to 9.4) and the product is obtained by extraction with MTBE and concentration by distillation. Compared to our previous publication,^[3] the stability and enantioselectivity of the enzyme was further improved by targeted enzyme engineering. Depletion of the enzyme was achieved by acidification and filtration of the precipitated denatured enzyme. However, hydrolysis of the product **6** under these acidic conditions and clogging of the filter complicated the enzyme removal. During development, we found that hydrolysis could be limited by tight control of the pH between 1.6 and 2.2. The filtration behavior of the denatured enzyme was improved by addition of MTBE (used for the extraction of the product) before filtration. Most likely, the added MTBE reduces the viscosity of the mixture by extraction and dilution of the product and by separating the oily product from the protein flakes, which tend to form a compact filter cake. Any remaining protein is then removed by a second filtration of the partially concentrated product solution. Protein content is controlled in the product **6** by the Bradford test. Another challenge was the formation of impurities upon concentration of the MTBE solution by distillation. Elucidation of the structure of the main side-product revealed that it was formed by hydrolysis followed by cyclization. Therefore, the distillation temperature was decreased to 60 °C to minimize the formation

of side-product **A**. Intermediate **6** was successfully manufactured on commercial scale producing ~11 tons of material with 40.4% yield, 97.5% w/w assay, 99.5 area% purity, and >98.0% ee (by GC analysis).

2.2 Formation of the Pyrimidine

The pyrimidine ring of the Ipatasertib core structure is formed by condensation of **6** with formamidine acetate (Scheme 2). Even though the reaction worked well throughout the clinical phases, process knowledge about the conversion kinetics with regard to scale-up requirements was limited since no standard analytical method (GC, HPLC) was able to measure both starting materials and product together. Additionally, quantification of the starting materials in the reaction mixture by GC gave very unreliable results. The process characterization studies to determine the proven acceptable ranges (PAR) were performed in a multivariate setup and conversion of **6** was followed by IR. It could be demonstrated that the reaction did not take more than 12 h for completion (7 h at set-point conditions, Fig. 3), which is the safe timeframe for routine manufacturing with regard to conversion, side-product formation and yield, without the need

for a routine in process control. Intermediate **7** was successfully manufactured on commercial scale producing ~8 tons of material with 78% yield, 99.95%w/w assay, and 99.9 area% purity (by HPLC analysis).



Scheme 2. Formation of the pyrimidine ring by condensation of **6** with formamidine acetate.

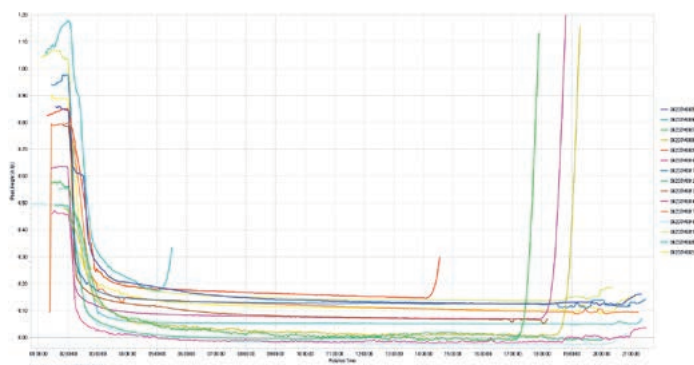


Fig. 3. Overlay of IR traces from multivariate experiments to follow the conversion of **6**.

2.3 Bromination of **7** and Coupling with *N*-Boc-Piperazine

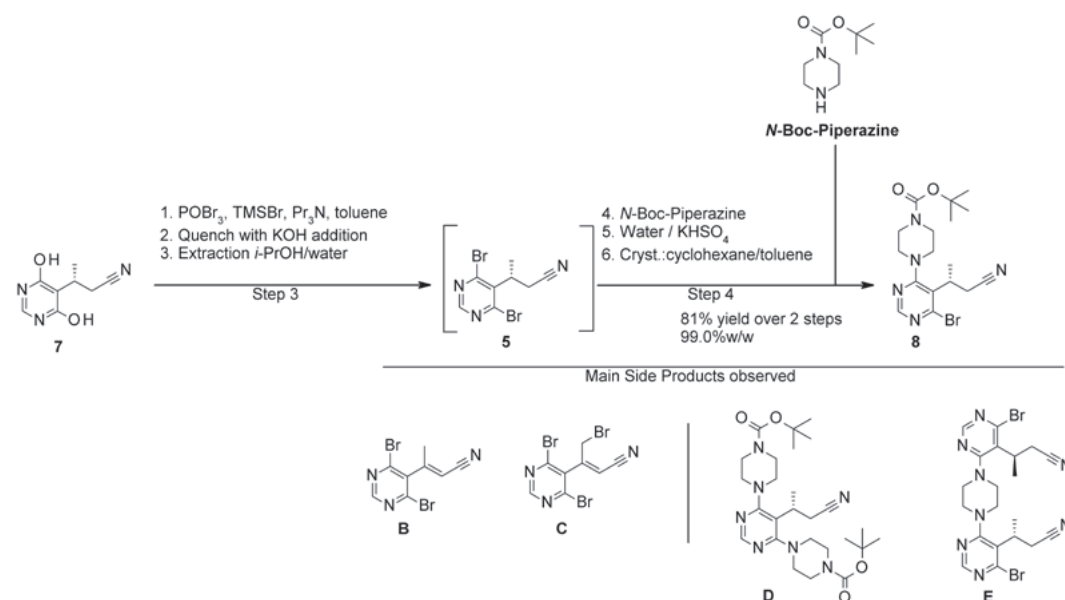
As reported in our previous publications,^[3-5] the di-brominated or iodinated intermediate **5** was produced by chlorination of in-

termediate **7** with POCl_3 to the dichlorinated pyrimidine and subsequent halogen exchange by either TMSBr or NaI . To avoid this laborious and resource intensive transformation, a direct bromination was investigated. While several brominating reagents (*e.g.* PBr_3 , $\text{HBr}/\text{Ac}_2\text{O}$, $\text{PPh}_3/\text{CBr}_4$, SOBr_2) delivered only small traces of **5**, finally a combination of POBr_3 and NPr_3 led to more promising results. However, the reaction mixture tended to become very viscous and crust formation was also an issue. Breakthrough was achieved by addition of TMSBr as an activation reagent for the hydroxyl groups of **7**, which also solved the viscosity and crust issue. Over-bromination leads to the formation of two impurities (**B** and **C**), which are increased at higher reaction temperature. Additionally, the reaction solvent toluene and the base NPr_3 are partially brominated to benzyl bromide and 1-propylbromide. As all brominated compounds formed in this reaction are potentially genotoxic, a more efficient control strategy was followed, controlling them with a limit test for bromine (max. 4 ppm by X-ray fluorescence) in intermediate **11**.

To further increase the process efficiency, we telescoped **5**, from the quenched reaction mixture, directly to a $\text{S}_{\text{N}}\text{Ar}$ reaction with *N*-Boc-piperazine to form intermediate **8** (Scheme 3). The auxiliary base NPr_3 remaining in the mixture containing **5** is sufficient to facilitate the $\text{S}_{\text{N}}\text{Ar}$ reaction. Double addition of *N*-Boc-piperazine to side-product **D** is controlled by stoichiometry (1.05 to 1.15 equiv. *N*-Boc-piperazine). Dimer **E**, formed by piperazine in *N*-Boc piperazine, showed unsatisfactory depletion and had to be controlled by limiting the amount of piperazine in *N*-Boc-piperazine to 0.20 area%. Intermediate **8** was successfully manufactured on commercial scale producing ~15 tons of **8** with 81% yield (over two steps), 99.0%w/w assay, and 99.3 area% purity (by HPLC analysis).

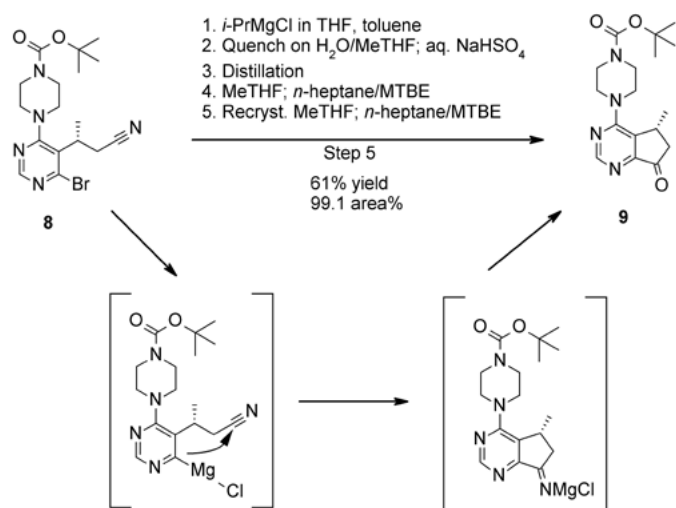
2.4 Formation of the Cyclopentyl Ring via Grignard Reaction

One of the key steps in the synthesis of Ipatasertib is the Grignard-induced cyclization of intermediate **8** to the bicyclic pyrimidine **9** (Scheme 4). For the development of this step, reaction conditions had to be optimized with respect to conversion rate, side-product formation, stability of the reaction mixture and color of the product. An intensive screening of various Grignard reagents (*i*-PrMgCl in THF and Et_2O , *i*-PrMgCl*LiCl in THF, *s*-BuMgCl*LiCl in THF, *t*-BuMgCl in THF) and reaction solvent (toluene, heptane, TBME, anisole, CPME, 2-MeTHF) combinations were tested. It was found that a certain amount of THF



Scheme 3. Telescoped bromination of **7** to **5** and subsequent $\text{S}_{\text{N}}\text{Ar}$ with *N*-Boc-piperazine to **8**.

seemed to be necessary to facilitate the reaction, since *i*-PrMgCl in Et₂O with toluene as reaction solvent showed significant amounts of residual starting material **8** (34%), after addition of the reagent, and more side-products were formed as well. On the other hand, with THF as reaction solvent mainly degradation was observed. For the reaction solvents, only toluene and anisole gave complete conversion and were similar with respect to impurity profile. In 2-MeTHF the conversion was slightly inferior and more side-products were observed. Toluene was then chosen as reaction solvent because it is removed more easily by distillation during the work-up than anisole.



Scheme 4. Grignard-induced cyclization of intermediate **8** to intermediate **9**.

As a compromise regarding all these aspects of product quality, we found the reaction fitting best in a combination of 3 L/kg (**8**) toluene as a reaction solvent, *i*-PrMgCl as Grignard reagent, and 7.5 °C reaction temperature. Under these conditions, the reaction is fast and controlled by the addition rate of *i*-PrMgCl, which first undergoes a bromide magnesium exchange with **8**, followed by fast intramolecular cyclization with the nitrile group to a cyclic imine. In a subsequent aqueous quench **9** is formed.

Furthermore, this step is a critical step for the color of the API. Although, there are three isolated intermediates between intermediate **9** and the API, colored impurities formed in this step have an impact on the color of the API. Therefore, the control of the color of intermediate **9** is of great importance.

The main side products in the reaction are **F**, **G**, and **H** (Fig. 4). **F** is formed continuously during the Grignard addition, whereas **G** seems to be formed from **F** with excess of Grignard reagent towards the end of the addition. **H** is mainly formed in the reaction mixture after complete Grignard addition. Besides the right choice of the Grignard reagent/reaction solvent combination, the concentration of the reaction contributed mainly to a clean conversion by decreasing the formation of impurities. In contrast to chemical intuition, the formation of dimeric side-products was suppressed by a more concentrated reaction mixture, most likely because at the start of the Grignard addition the majority of the starting material **8** is not yet dissolved. Therefore, the amount of reaction solvent was decreased.

Another challenge of this reaction was the work-up. Due to the limited stability of the reaction mixture, it has to be quenched immediately after completed addition of the Grignard reagent to avoid the formation of side-products and colored impurities. The quench is done by simultaneous addition of the reaction mixture and aqueous NaHSO₄ onto a mixture of 2-MeTHF and water.

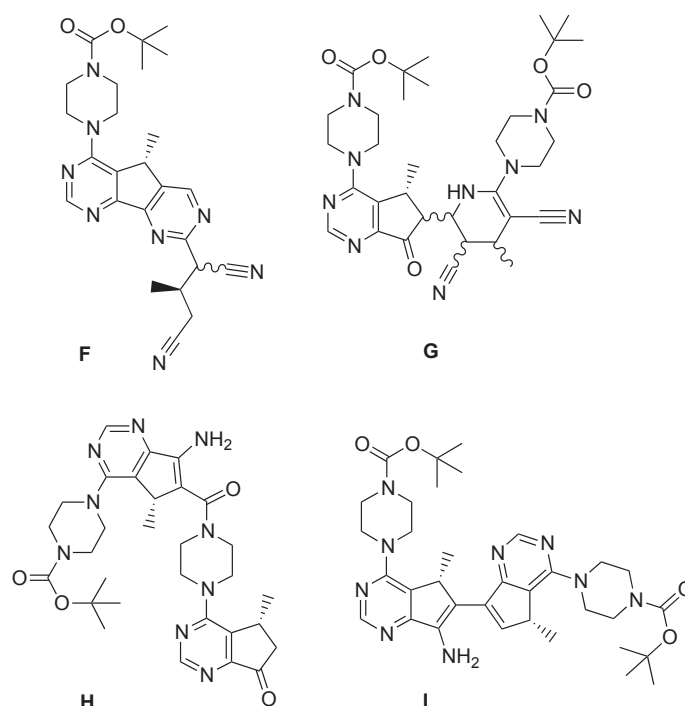


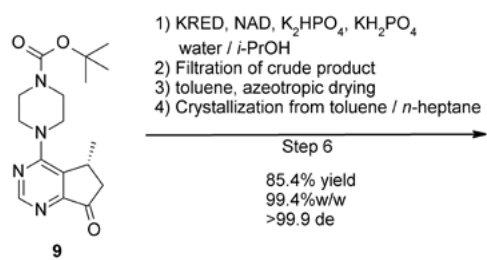
Fig. 4. Main side-products formed in the Grignard-induced cyclization.

In the early phase development, a pH range of 3.5 to 5.0 was deemed optimal to prevent cleavage of the boc-protecting group and to hydrolyze the cyclic imine. However, it was difficult to keep the pH in that range with a simultaneous addition and NaHSO₄ as proton source. An experiment using a citric acid buffer to keep the pH at ~4 led to the unexpected formation of ~20% of side-product **I**. After such an unexpected result within the established pH range, the addition of the reaction mixture on 40%w/w aqueous NaHSO₄ was also tested. To our surprise, the product was quite stable at that low pH (< 1) at 0 °C. Based on this result, we optimized the quench to a parallel addition of the reaction mixture and 40%w/w NaHSO₄ on water at pH 1.5 to 2.5 and subsequent pH adjustment with 2M NaOH to 4.0 to 5.5 to keep the product in the organic phase. By using a mixture of water and 2-MeTHF the immediate removal of the product from the acidic aqueous phase improved the product quality. As an important side effect, ether type solvents (like 2-MeTHF) helped to remove color from the product. Therefore, and to avoid crust formation, a mixture of *n*-heptane and MTBE was used to crystallize the product. The obtained crude **9** was then slurried in 2-MeTHF and precipitated by *n*-heptane/MTBE for further purification and removal of colored impurities. With that process, intermediate **9** was successfully manufactured on commercial scale producing ~5.5 tons material with 61% yield, and 99.1 area% purity (by HPLC).

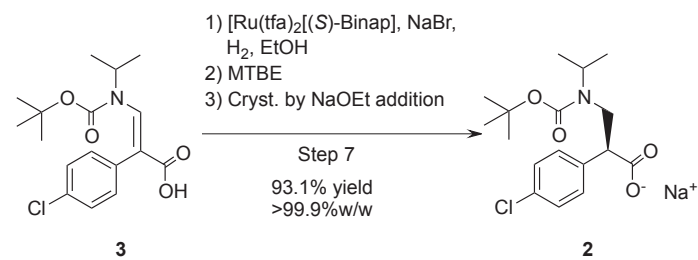
2.5 Second Enzyme Catalysis – Introduction of the Second Stereo Center

The second stereo center was introduced by absolute diastereoselective reduction of the keto function in intermediate **9** with an engineered ketoreductase and *i*-PrOH as hydrogen source and NAD as co-factor (Scheme 5).

The reaction is performed in water with 3.5 equiv. of *i*-PrOH, so only a small amount of starting material and product are dissolved, allowing a rather concentrated reaction. The reaction operates well in a range of 4 to 12 L of water per kg of intermediate **9**. In the latest optimizations of this step, an evolved enzyme was introduced, reducing the reaction time with the same enzyme load from ~60 h to ~20 h (conversion >99.0%). The crude product is then filtered off, washed with water, dissolved in toluene, and



Scheme 5. Stereoselective reduction of intermediate **9** by an optimized ketoreductase.



Scheme 6. Stereoselective hydrogenation of starting material **3** with ruthenium catalyst.

dried by azeotropic distillation in order to remove the remaining enzyme by filtration. Finally, intermediate **4** is crystallized by *n*-heptane addition. Residual protein is controlled again by Bradford test of the isolated intermediate **4**.

With the initial crystallization protocol (addition of *n*-heptane at 25 °C, seeding, and then cooling to −10 °C), oiling was observed which resulted in crust formation. Additionally, analysis of our manufacturing data revealed that the crystallization was influenced by the content of residual water in the toluene solution. With that, an improved process was developed, where 1 equiv. of water is added and the order of the process steps was changed (cooling to −10°C, seeding, then addition of *n*-heptane). The effect of the water was nicely demonstrated in one experiment where the stirring speed was set to a too low rate and frozen water droplets accumulated below the stirrer. The crystal growth did mainly take place at these droplets. With that process, intermediate **4** was successfully manufactured on commercial scale producing ~5 tons of material with 85.4% yield, 99.4%w/w assay, 99.8 area% purity, and >99.9%de (by HPLC analysis).

2.6 Formation of the Third Stereo Center by Ruthenium Catalyzed Hydrogenation

The last stereo center is introduced by stereo selective hydrogenation of starting material **3** with a highly active and selective ruthenium catalyst (Scheme 6). The chosen catalyst for the asymmetric hydrogenation of **3** entails several advantages. The synthesis of the catalyst was developed at Roche in the late 1980s and published in 1991.^[6] However, no supply chain for large-scale production was available when we started our work. Therefore, we revised and optimized the catalyst synthesis to enable kg amount supply by a contract manufacturing organization (CMO). This ensured high catalyst quality and a smooth transfer of the process to commercial manufacturing scale.

The catalyst can be applied at a high *s/c* (substrate/catalyst) ratio of up to 10000 (mol/mol) and is activated with NaBr.^[3] As a

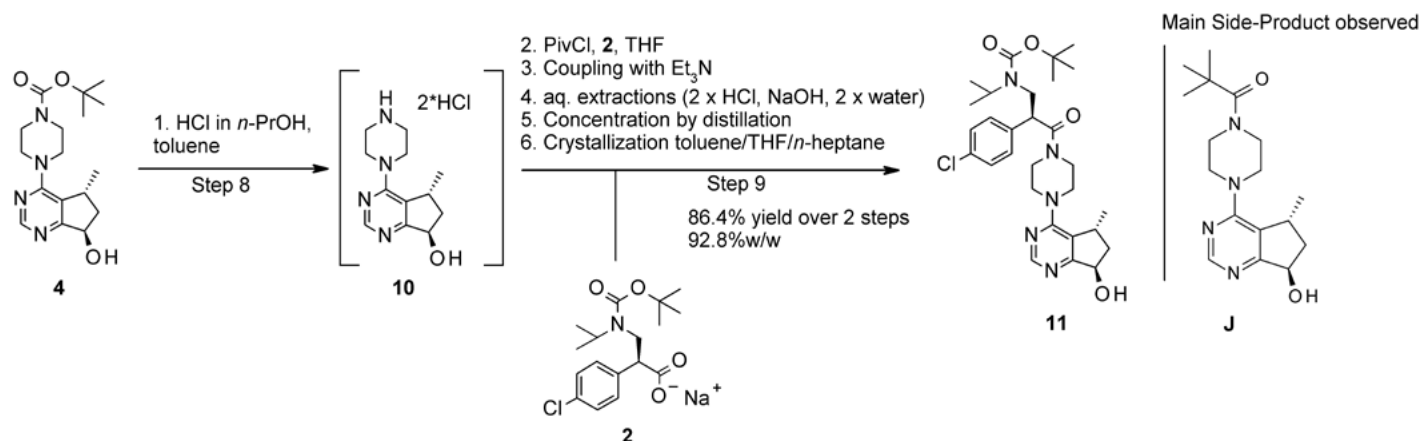
consequence of the very low catalyst loading the reaction is sensitive towards temperature, hydrogen pressure and dilution. In the multivariate experiments to determine the PAR, it was observed that the conversion becomes incomplete with a combination of low catalyst loading (*s/c* = 5000, tested range *s/c* = 4000 to 5000), low hydrogen pressure (10 bar, tested range 10 to 20 bar), and high dilution 11.82 g/g (**3**) ethanol, tested range for ethanol 7.88 to 11.82 g/g (**3**). Therefore, the catalyst loading for the routine manufacturing process was set to *s/c* 4000. The product **2** is then isolated as a sodium salt by addition of MTBE and NaOEt. The small amounts of residual ruthenium are efficiently removed by the crystallization (<3 ppm).

Due to the relatively large manufacturing amounts, the low bulk density of ~0.1 kg/L was limiting the throughput of the dryer. Therefore, an adapted crystallization procedure was developed increasing the bulk density by more than factor 3 to 0.35 kg/L. In the improved process, seed crystals are generated by the addition of 0.20 equiv. NaOEt (just enough to start the nucleation) and aged for 2 h, followed by another 1 equiv. NaOEt to complete the crystallization. With that process, intermediate **2** was successfully manufactured on commercial scale producing ~5.5 tons of material with 93.1% yield, >99.9%w/w assay, 100 area% purity (by HPLC analysis), and >99.9%ee (by chiral HPLC analysis).

2.7 Coupling of Intermediates 2 and 4

Both key building blocks **2** and **4** are then coupled in the next step to yield Boc-protected API **11** (Scheme 7). **4** is first deprotected with HCl in *n*-propanol to yield **10**, followed by free-basing with Et₃N. In a second reaction **2** is activated with pivaloyl chloride, which is then coupled with **10** to form intermediate **11**.

The initially applied process using propylphosphonic anhydride (T3P) as coupling reagent and *N*-methylmorpholine as base, suffered from incomplete conversion, leaving about 5–7% of the valuable intermediate **4** unreacted in a very viscous reaction mixture resulting in only 75% yield. Additionally, aqueous waste



Scheme 7. Deprotection of **4** followed by coupling with activated **2** to yield Boc-protected API.

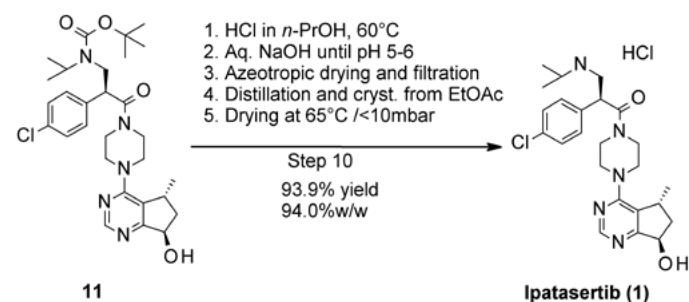
streams, with a too high phosphorous content for the wastewater treatment plant needed to be incinerated. An intensive screening of coupling reagents for the activation of **2** (CDI, FDPP, PivCl, EDC, NSC, Ph₃POCl, thionyl chloride, oxalyl chloride, isobutylchloroformate, sec-butylchloroformate) revealed that pivaloyl chloride in toluene as reaction solvent gave the most promising initial results. However, several scale-up experiments showed that with these process conditions no reproducible results could be obtained. Classical HPLC or GC analytics to monitor the activation of **2** failed to show reliable results. Thus, by utilizing an online IR probe, it was possible to monitor the pivaloyl chloride conversion and formation of activated **2**. Monitoring the activation of **2** in toluene by IR confirmed the large difference in activation performance. Eventually, THF was tried as reaction solvent leading to a relatively fast and reproducible activation. IR trends of one activation experiment are shown in Fig. 5.

In order to evaluate the robustness of this newly developed process a number of selected process parameters were assessed in a screening DoE (Plackett Burman 12 design). A four factor interaction of substoichiometric amounts of pivaloyl chloride with respect to **2**, a high concentration of the reaction (4 g/g (**2**) THF) and an increased reaction temperature of 30 °C, was found to lead to about 50% epimerization at the stereo center of **2**. This example shows how important multivariate experimentation at an early development point can be. Without that, we would have never been able to detect that critical parameter interaction, bearing the risk of a failed batch in manufacturing. Therefore, the parameter ranges of pivaloyl chloride and **2** were set to 1.10 to 1.15 equiv. and 1.025 to 1.075 equiv. respectively, which ensures excess of pivaloyl chloride with respect to **2**. The reaction solvent amount was also set slightly higher, allowing 5.0 to 7.0 kg/kg (**4**) for THF. The reaction temperature was lowered to -10 to 10 °C, because also at this lower temperature the reaction time with maximum 17 h was still acceptable. Following the IR trends for **2** in manufacturing showed very consistent reaction performance (Figs 6 and 7).

Work-up of the reaction mixture is done by concentration by distillation, followed by acidic, basic, and neutral aqueous extractions to deplete unreacted pivaloyl chloride, residual **2**, and the main side-product **J** formed in the process. Side-product **J** is observed in the reaction mixture with approximately 5 area% but is completely depleted in the work-up. With this improved process, intermediate **11** was successfully manufactured at commercial scale producing ~7 tons of material with 86.4% yield, 92.8%w/w assay, and 99.8 area% purity (by HPLC analysis).

2.8 Deprotection to Ipatasertib (**1**) and Spray Drying

In the final chemical transformation, intermediate **11** is deprotected by HCl in *n*-propanol (Scheme 8). The mono-HCl form of Ipatasertib is obtained by titration to pH 5 to 6 (the equivalence point) with aqueous NaOH. Water is removed from the reaction mixture by distillation to allow the complete removal of NaCl by filtration. Furthermore, the product is precipitated by removal of *n*-propanol by distillation and addition of ethyl



Scheme 8. Deprotection of intermediate **11** to yield Ipatasertib (**1**).

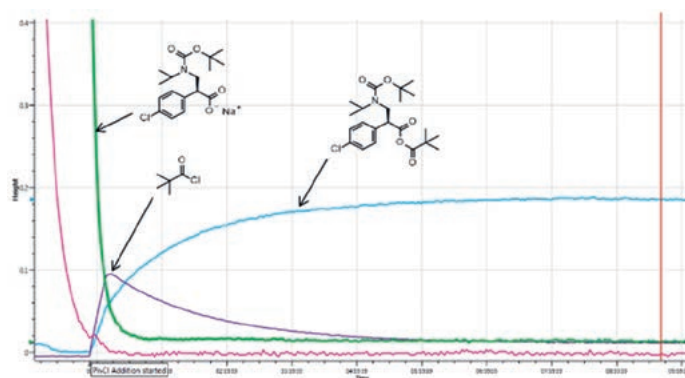


Fig. 5. IR trends for the activation of intermediate **2** with pivaloyl chloride.

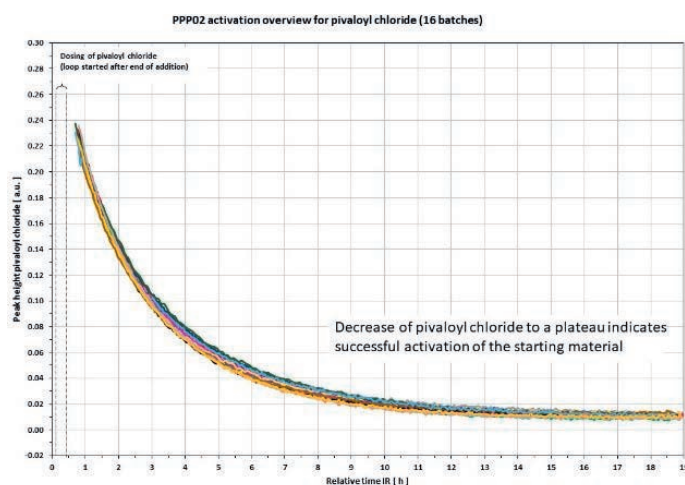


Fig. 6. IR trend for pivaloyl chloride of 16 manufacturing batches used in the activation of intermediate **2**.

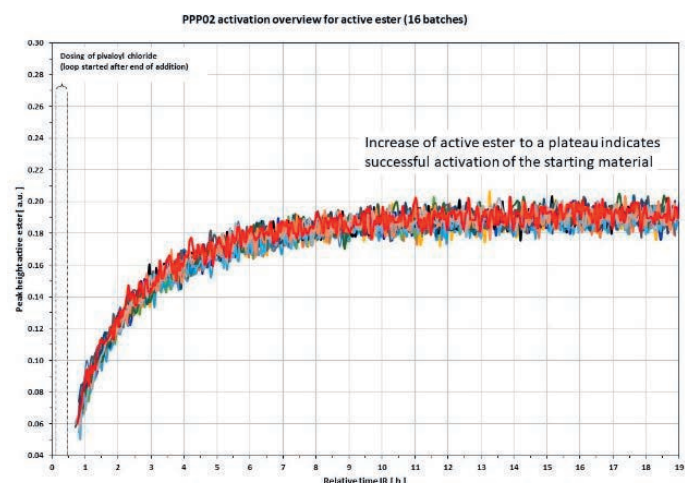


Fig. 7. IR trend for activated-**2** of 16 Manufacturing Batches used in the Activation of Intermediate **2**.

acetate. Ipatasertib (**1**) is obtained after drying as partially amorphous material with 5 to 8% ethyl acetate content. This step was successfully manufactured on commercial scale producing ~5.5 tons of material with 93.9% yield, 94.0%w/w assay (by HPLC; 6.4% ethyl acetate). To obtain the selected amorphous form of the API and to adjust the particle size distribution for galenical manufacturing **1** is spray dried as aqueous solution with a typical yield of 95%.

3. Summary

In the course of our late stage development, the implemented process improvements led to a decrease of the mass intensity factor (kg / kg API) over the last three campaigns from 1393, over 462, to 269 for the commercial process. This is a reduction by factor 5 and a rather low MI for such a sophisticated and long reaction sequence (Fig. 8). The overall yield was improved by factor 3 from 2.9%, over 9.3%, to 9.7% (24% if excluding the kinetic resolution in step 1).

The process uses mainly ecofriendly solvents such as water, ethanol, and ethyl acetate (Fig. 9). Solvents of concern, such

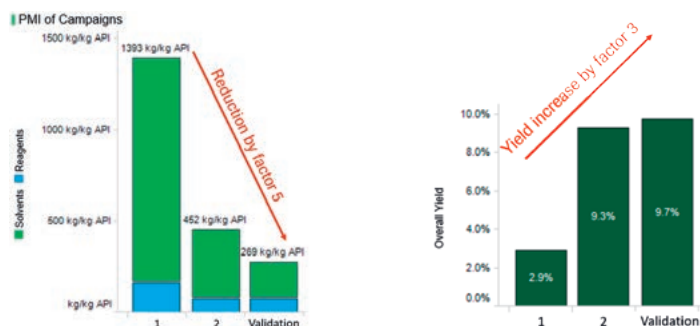


Fig. 8. Mass intensity and yield improvements over the last three manufacturing campaigns

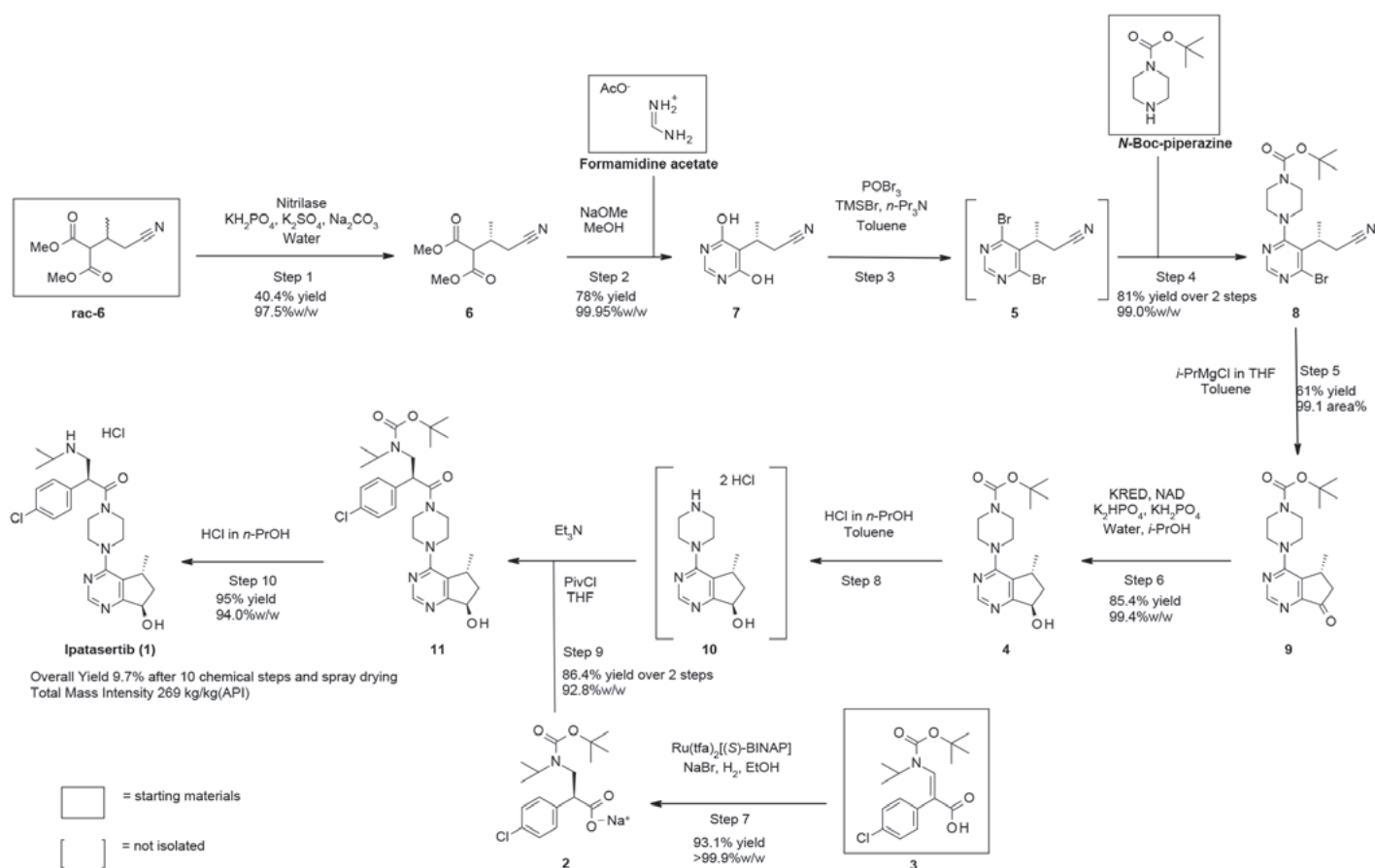
as DMF, DMA, DCM, or NMP were substituted during process development. Additionally, most solvent waste streams are recycled to further minimize the ecological footprint of the manufacturing process.

Overall, the commercial manufacturing process for Ipatasertib is highly efficient and sustainable. Furthermore, the process performance and robustness has been successfully proven at commercial scale over all ten chemical steps and the final spray-drying step (Scheme 9). For the manufacturing of this complex compound, a wide range of chemical reaction types and techniques such as on-line IR monitoring, spray drying, bio and metal catalysis, and various reaction classes like condensation (with formamidine), bromination, Grignard reaction, and amide formation are used.

Acknowledgements

Alfred Stutz, Annabarbara Fiess, Beat Wirz, Catherine Bisch, Christian Kuzniewski, Christian Mössner, Daniel Zingg, Debora Manns, Franziska Lange, Georg Wuitschik, Gino Semadeni, Henriette Arndt, Jannik Martin, Johannes Burkhard, Katrin Oehring, Klaus-Daniel Umland, Luca Weber, Manuela Erni, Manuela Hofmann, Manuela Keller, Marc Wermelinger, Martin Mehlmann, Martina Bütikofer, Michelangelo Scalone, Manuela Müller, Pascal Müller, Patrick Meier, Arthur Meili, Pirmin Hidber, Reinhard Reents, Roger Schätti, Daniel Speiss, Markus Steiner, Severin Stocker, Tatjana Becherer, Tomohiro Oki, Viktor Hoffmann.

Received: May 20, 2021



Scheme 9. Overview of the Ipatasertib (1) synthesis.



Fig. 9. Amount and type of solvents used in the last three manufacturing campaigns. Size of the pie chart represents the amount of solvents used.

Preferred: Toluene, water, EtOH, MeTHF, Acetic Acid

Usable: THF, MTBE, MeOH, Heptane, Cyclohexane, Acetonitrile, 2-PrOH

Undesired: DMF

- [1] B. D. Manning, L. C. Cantley *Cell* **2007**, *129*, 1261, <https://doi.org/10.1016/j.cell.2007.06.009>
- [2] J. F. Blake, R. Xu, J. R. Bencsik, D. Xiao, N. C. Kallan, S. Schlachter, I. S. Mitchell, K. L. Spencer, A. L. Banka, E. M. Wallace, S. L. Gloor, M. Martinson, R. D. Woessner, G. P. A. Vigers, B. J. Barndhuber, J. Liang, B. S. Safina, J. Li, B. Zhang, C. Chabot, S. Do, L. Lee, J. Oeh, D. Sampath, B. B. Lee, K. Lin, B. M. Liederer, N. J. Skelton, *J. Med. Chem.* **2012**, *55*, 8110, <https://doi.org/10.1021/jm301024w>
- [3] C. Han, S. Savage, M. Al-Sayah, H. Yajima, T. Remarchuk, R. Reents, B. Wirz, H. Iding, S. Bachmann, S. M. Fantasia, M. Scalone, A. Hell, P. Hidber, F. Gosselin, *Org. Lett.* **2017**, *19*, 4806, <https://doi.org/10.1021/acs.orglett.7b02228>
- [4] J. W. Lane, K. L. Spencer, S. R. Shakya, N. C. Kallan, P. J. Stengel, T. Remarchuk, *Org. Process Res. Dev.* **2014**, *18*, 1641, <https://doi.org/10.1021/op500271w>
- [5] T. Remarchuk, F. St-Jean, D. Carrera, S. Savage, H. Yajima, B. Wong, S. Babu, A. Deese, J. Stults, M. W. Dong, D. Askin, J. W. Lane, K. L. Spencer, *Org. Process Res. Dev.* **2014**, *18*, 1652, <https://doi.org/10.1021/op500270z>
- [6] B. Heiser, E. A. Broger, Y. Crameri, *Tetrahedron: Asymmetry* **1991**, *2*, 51, [https://doi.org/10.1016/S0957-4166\(00\)82157-6](https://doi.org/10.1016/S0957-4166(00)82157-6)

License and Terms



This is an Open Access article under the terms of the Creative Commons Attribution License CC BY 4.0. The material may not be used for commercial purposes.

The license is subject to the CHIMIA terms and conditions: (<http://chimia.ch/component/spagebuilder/?view=page&id=12>).

The definitive version of this article is the electronic one that can be found at <https://doi.org/10.2533/chimia.2021.605>